Controlling X-rays With Light

T.E. Glover[1], M.P. Hertlein[1], S.H. Southworth[2], T.K. Allison[3,1], J. van Tilborg[1], E.P. Kanter[2], B. Krässig[2], H.R. Varma[2], B. Rude[1], R. Santra[2,4], A. Belkacem[1], and L. Young[2*].

[1]Lawrence Berkeley National Laboratory, Berkeley CA 94720, USA

[2]Argonne National Laboratory, Argonne IL 60439, USA

[3]Department of Physics, University of California, Berkeley CA 94720, USA

[4]Department of Physics, University of Chicago, Chicago IL 60637, USA

[*]e-mail: young@anl.gov

ABSTRACT

Ultrafast x-ray science is an exciting frontier that promises the visualization of electronic, atomic and molecular dynamics on atomic time and length scales. A largely unexplored area of ultrafast x-ray science is the use of light to *control* how x-rays interact with matter. In order to extend control concepts established for long wavelength probes to the x-ray regime, the optical control field must drive a coherent electronic response on a timescale comparable to femtosecond core-hole lifetimes. An intense field is required to achieve this rapid response. Here an intense optical control pulse is observed to efficiently modulate photoelectric absorption for x-rays and to create an ultrafast transparency window. We demonstrate an application of x-ray transparency relevant to ultrafast x-ray sources: an all-photonic temporal cross-correlation measurement of a femtosecond x-ray pulse. The ability to control x-ray/matter interactions with light will create new opportunities at current and next-generation x-ray light sources.

To date, ultrafast x-ray science has focused on using x-rays as weakly-interacting, linear probes to measure structural changes with atomic spatial resolution on the picosecond to femtosecond timescale; see for example [1-3]. Ultrafast x-ray absorption spectroscopy, with its sensitivity to local electronic and atomic structure, has been used to track light-induced molecular dynamics in solution [3-5] as well as electronic dynamics in solids [1]. More closely related to the current work are experiments in the gas phase which use x-ray absorption to probe ionized atoms [6,7] or laser-aligned molecules [8]. Orbital-hole alignment, coupling between valence and core wavefunctions, and controlled x-ray absorption from laser-aligned molecules are effects which have been observed in these latter experiments. All of these examples use light to modify the target system and x-rays to *monitor* the response.

In this work, we use light for a fundamentally different purpose – to *control* x-ray interactions with matter. We accomplish this by using optical radiation to modify the short-lived core-excited states accessed by x-ray absorption. Our work is inspired by quantum optics studies at longer wavelengths that use light to couple selected excited states of a material which is in its ground state. The ability to induce transparency, enhance nonlinear scattering, and bring light to a near standstill are examples of such control effects which, to date, have principally used long wavelength resonance radiation for both control and probe pulses [9-11]. Recently, an extension of optical control to the extreme ultraviolet regime was reported [12]. An analogous ability to control x-ray/matter interactions with light would create new opportunities at existing and next-generation x-ray facilities which promise ultrafast, intense, coherent x-ray radiation [13-

15]. On the picosecond timescale, control of x-ray beams has been previously demonstrated using laser-driven impulsive excitation of acoustic phonons in a crystal lattice [16] and piezoelectrically induced lattice distortion in a thin film [17]. On a femtosecond timescale, the ability to shape the temporal profile of an x-ray pulse by modulating absorption, as previously proposed [18], would facilitate extension of coherent-control schemes to the x-ray regime, in analogy to longer wavelength experiments that use shaped electromagnetic pulses to drive a system along a specified dynamical pathway [19]. Similarly, *nonlinear* x-ray spectroscopy is a promising frontier enabled by next-generation light sources [20]. The cross-sections for nonlinear scattering at short wavelength are intrinsically weak and a route to tailoring these cross sections is desirable.

Extension of optical control to the x-ray regime is complicated by the short-lived nature of core-excited states. Femtosecond core-hole lifetimes make it impossible to maintain coherence among the core-excited states over multiple optical cycles. Furthermore, to compete with rapid population decay one must use an intense control beam, one that is sufficiently intense to induce transitions (Rabi flopping) between core-excited Rydberg states on a timescale faster than their decay (typically a few femtoseconds). This introduces two complications. First, ionization becomes important. The coupling field strength cannot be arbitrarily increased in an attempt to combat core-hole decay since destruction of the ground state via ionization will ensue. For the system studied in this work, gaseous neon, the Rabi flopping period (~1-fs) is comparable to the core-hole lifetime (2.4 fs) for an 800-nm coupling laser at ~10^{13}

W/cm^2; an intensity which leaves the ground state unperturbed yet rapidly ionizes the optically-coupled core-excited Rydberg states. Since the final states of the x-ray transition are coherent superpositions of these rapidly ionizing states, a fundamental question arises – that of the very existence of quasi-resonant inner-shell absorption structures in the presence of intense optical control fields. As a second issue, optical couplings among several series of core-excited Rydberg states and continua become important, so the few-level models typically used to demonstrate control at longer wavelengths become inadequate. These issues introduce fundamental uncertainties about whether intense optical pulses can efficiently modulate x-ray transitions.

It is this new and unique regime of coherent strong coupling between short-lived core-excited states that we explore in order to achieve active optical control of x-ray absorption. A femtosecond optical pulse is observed to efficiently and reversibly induce transparency in a gaseous medium nominally opaque to x-rays. An ultrashort transparency window is created which dramatically increases, by a factor of three, the transmission of a femtosecond x-ray probe pulse. This transparency is most efficiently induced when the linearly polarized optical and x-ray pulses are polarized parallel to one another. Our observations demonstrate that in spite of rapid population decay inherent to core-excited states, intense optical pulses can be used as tools to efficiently control x-ray absorption. We demonstrate an application relevant to ultrafast x-ray sources by performing an all-photonic measurement of a femtosecond x-ray pulse profile.

Optical control of x-ray absorption in neon

We chose gaseous neon to study optical control of x-ray transitions. Neon has a high ionization potential (21.6 eV), making it resistant to optical strong field ionization and permitting a wide range of control pulse intensities without destruction of the medium. Neon 1s core-hole states have a 2.4-fs lifetime (natural linewidth $\Gamma \sim 0.27$ eV), requiring control pulse intensities of 10^{13} W/cm^2. The laser-induced x-ray transparency may be understood heuristically as a single active electron within a coupled three-level Λ system ($1s \rightarrow 1s^{-1}3p \Leftrightarrow 1s^{-1}3s$) where a weak x-ray field (ω_X) probes the $1s \rightarrow 1s^{-1}3p$ core-to-Rydberg transition and a strong laser field (ω_L) couples the core-excited $1s^{-1}3p$ and $1s^{-1}3s$ states. Prior studies [18] predict enhanced transparency for the x-ray probe transition ostensibly as a result of coupling between the $1s^{-1}3p$ and $1s^{-1}3s$ states, states henceforth referred to as 3p and 3s. With Ω_R as the Rabi frequency and τ_L the laser period, the relevant timescales are $\tau_L = 2.8$ fs, $1/\Omega_R \sim 1$ fs and $1/\Gamma = 2.4$ fs. In reality, the situation is more complex as illustrated in Figure 1. In the absence of the laser field, x-ray absorption from the 1s level accesses the np manifold (Fig. 1a) creating the well-known Rydberg series as a function of x-ray energy. However, in the presence of the strong coupling field (red arrows in Fig. 1b) both strong mixing of the core-excited nl Rydberg levels and laser-induced ionization become important. While the relative strength of the mixing between specific nl states is governed by the detuning of the coupling laser ω_L from the field-free resonance energies, mixing is unavoidable and pervasive for core-excited Rydberg states with large inherent widths and additional laser-induced widths. This creates a more complex situation than is typical for longer wavelength optical control experiments [9-11] where a few-level subspace can be readily

identified since the coupling laser energy, ω_L, is large relative to energy widths due to population decay, Γ, and Rabi flopping Ω_R.

The measured laser-free x-ray absorption spectrum in the vicinity of the neon K-edge is shown in Fig. 2 along with several relevant atomic states. X-ray excitation of a 1s electron to the 3p orbital gives rise to the strong resonance at 867.1 eV and we seek to induce transparency on this transition via coherent coupling of the 3s and 3p core-excited states.

Observation of transparency

Co-propagating, focused x-ray and 800-nm optical pulses overlap in a gas cell in four-dimensions (3 spatial and 1 temporal). We gate the detection electronics to sequentially record laser-on and laser-off x-ray transmission spectra and scan the x-ray energy. Laser induced changes to the transmission spectra are shown in Fig. 3, which plots the fractional change in transmission. Spectra are shown for a range of intensities (up to ~2x) and for a control beam polarized parallel to the x-ray probe. The laser dramatically enhances x-ray transmission at the laser-free absorption maximum. At the highest intensity the measured x-ray transmission is increased by a factor of three. The observed variation of transparency with laser intensity is linear within error. Notably, the transparency induced on line-center is accompanied by induced absorption, evidenced as absorption peaks to either side of line-center. At the highest intensity, the high (low) energy absorption peak is spaced ~ 0.7 eV (0.6 eV) from line-center. The observed degree of transparency, while large, is limited by experimental considerations

such as non-uniform laser intensity over the gas medium, and finite x-ray energy resolution. *Ab initio* calculations [18] indicate that for an ideal situation with a spatially and temporally uniform coupling laser intensity of $1x10^{13}$ W/cm^2, the resonant x-ray absorption cross section is decreased by a factor of ~13.

To gain insight into the underlying mechanism of the observed transparency, the dependence on laser polarization was studied. These studies were performed at half the neon density used for Fig. 3. The results for the parallel (upper panel) and perpendicular (lower panel) configurations are shown in Fig. 4. A dramatic decrease in transparency is observed when the polarization is switched from parallel to perpendicular. Transparency is almost eliminated for perpendicular polarization, which shows a factor of ~5 reduction in transparency.

The observed polarization dependence indicates that a three-level subspace (1s-3p-3s) has been, in our experiment, isolated by the judicious choice of the polarization ($\boldsymbol{\varepsilon}_L$) and energy ($\omega_L$) of the strong coupling laser. The x-ray couples the 1s state to the 3p, m_l=0 state, where the x-ray polarization vector $\boldsymbol{\varepsilon}_X$ defines the quantization axis. For the parallel configuration of laser and x-ray polarizations ($\boldsymbol{\varepsilon}_L \| \boldsymbol{\varepsilon}_X$), the laser can couple the 3p, m_l=0 state to the ns manifold, whereas in the perpendicular configuration ($\boldsymbol{\varepsilon}_L \perp \boldsymbol{\varepsilon}_X$) laser-mediated coupling to the ns manifold is symmetry-forbidden. Within the ns manifold, the 3s-3p coupling is dominant; the coupling laser (ω_L=1.55 eV) is resonant with the neon 3s-3p energy splitting (ΔE=1.88 eV) [21] within their broadened natural/laser-induced linewidths (Γ_{3s}~0.54 eV, Γ_{3p}~0.68 eV) [18]. In reality, 3p-nd and higher-order couplings are also present in the system, but the ns-manifold, and in

particular the 3s-3p coupling, is the key interaction underlying the observed polarization dependence of the x-ray transparency.

This conclusion is supported by our *ab initio* simulations of the transmission of x-rays through the laser-dressed neon medium that account for the non-uniform laser-coupling intensity experienced by the x-ray pulse (for details see Methods). The simulations (solid lines in Figs. 3 & 4) do an excellent job reproducing the essential features of the transmission spectra as well as the observed dependencies on control-pulse intensity and polarization. The simulated spectra were computed using *no adjustable parameters*. For insight, calculated absorption cross sections [18,22] for parallel and perpendicular configurations are shown in Fig. 4b for a uniform dressing laser intensity of 10^{13} W/cm^2. They confirm the strong dependence of transparency on polarization shown in Fig. 4a. The $\boldsymbol{\varepsilon}_L||\boldsymbol{\varepsilon}_X$ configuration exhibits a strong laser-induced transparency on the 1s → 3p line center, whereas the $\boldsymbol{\varepsilon}_L\perp\boldsymbol{\varepsilon}_X$ configuration shows no such dip at the line center. In calculations in which coupling to ns core-excited states is removed, we find that the cross sections are relatively insensitive to polarization. From these measurements and calculations we conclude that 3s-3p coupling underlies the observed transparency. However, we note that while the origin of the polarization dependence is clear, the magnitude of the induced transparency cannot be reproduced in *ab initio* calculations where we restrict the set of core-excited Rydberg states to 3s and 3p only.

Relationship to coherence effects in the optical domain

We next discuss the observed spectral modifications, due to strong coherent coupling between the 3p and 3s core-excited states, in relation to two effects extensively studied in the long wavelength regime: the Autler-Townes effect [10,23], and electromagnetically induced transparency (EIT) [9,10] . In the Autler-Townes effect a resonance line (1s→3p) in a coupled three-level system splits into two symmetric lines in the presence of a resonant coupling field (3s⇔3p). The currently observed spectral modifications are more complex. An analysis of the *ab initio* spectra for the $\boldsymbol{\varepsilon_L}||\boldsymbol{\varepsilon_X}$ configuration indicates a sequence of couplings with more than 10 (40) spectral resonances contributing to the transparency peak (full spectrum).

Laser-induced ionization contributes an additional width, and it is not self-evident that a resonant x-ray absorption structure should exist at our high optical intensity. At our peak laser intensity ~10^{13} W/cm^2 the 3s and 3p states do not even exist within a classical model of ionization. In a simple static-field model [24], an electron with binding energy W is bound only when $W \geq 2\sqrt{F}$ where F is the static field strength. For W=0.1 au, the 3p binding energy, the electron is classically bound only at field strengths below F=0.0025 au; a range of strengths which, at our peak intensity, exists over only 10% of an optical cycle. Our observation of resonant structure represents an unusual and new strong-field regime for the formation of Autler Townes-like doublets.

We also comment on the role of quantum interference (QI) and electromagnetically induced transparency (EIT) in the observed spectra [9,10]. EIT typically couples two long-lived states with a single upper state in a Λ configuration, whereas here we have two short-lived states (3s and 3p) coupled to the ground state.

QI becomes important when the upper Λ state (3p) is short-lived compared to the others (3s, 1s) [10,25,26]. In principle, coupling-laser-induced ionization may allow the QI mechanism at the heart of EIT to play a role if the lifetime of the upper Λ state can be significantly shortened with respect to the others. One might expect that this condition would be fulfilled since the upper Λ state is more weakly bound and should therefore be preferentially ionized. A more careful analysis, however, indicates that QI plays a rather modest role. Specifically, without QI, the absorption cross section from the 1s state is simply the sum of two noninterfering Lorentzians. In order to assess the role of QI in our strong-field regime, we identified in *ab initio* calculations ($\boldsymbol{\varepsilon}_L \| \boldsymbol{\varepsilon}_X$, 1×10^{13} W/cm^2) all dressed-state resonances contributing to the x-ray absorption cross section between 865 eV and 870 eV. Using these selected resonances, we evaluated the x-ray absorption cross section with and without the interference terms. At the 1s-3p resonance, the calculated cross sections were found to agree with each other to within a few percent. Accordingly, the contribution of QI to the transparency effect observed here is relatively small: in the spectral range of interest, the x-ray absorption cross section is essentially a sum of noninterfering Lorentzians.

The x-ray regime, however, does allow some simplifications relative to the optical regime. The coupling laser need only be quasi-monochromatic because level widths ensure resonance over a wide range of coupling laser energies. Coherence properties of the coupling laser are unimportant over multiple cycles. Finally, dephasing mechanisms for the atomic coherence, such as collisions, are unimportant here due to the rapid femtosecond core hole decay.

X-ray pulse measurement

We conclude by applying laser-induced transparency to characterize the femtosecond x-ray pulse duration. An x-ray/optical cross-correlation is obtained by tuning x-rays to the laser-free absorption maximum and then measuring the transmitted x-ray flux as a laser pulse (parallel polarization) is scanned in time across the x-ray pulse. The laser temporal duration (~290 fs), as determined by autocorrelation using second harmonic signal in a Michelson geometry, and the cross correlation width (~380 fs, Fig. 5) indicate an x-ray duration of ~250 fs +(-) 65(110) fs. Here we have assumed a linear dependence of transparency on intensity and the error bars on the pulse measurement reflect the departure from linearity allowed by the error bars of Fig. 3. The modulation of the x-ray interaction cross-section is essentially instantaneous on the ~100 fs timescale of the current pulses, and the measured x-ray duration is consistent with that expected (~225 fs) from simulations of the x-ray generation process [27]. With this said, we note that simulations indicate that care must be taken when extracting pulse profiles since nonlinearities can arise from the intensity dependence of the cross section as well as from strong absorption through the gas cell. The current approach to x-ray pulse measurement is potentially simpler than approaches based on photoelectron spectroscopy [28], where high performance photoelectron spectrometers are needed, and should prove helpful to developing ultrafast x-ray science at next generation light sources.

Summary and outlook

In summary, we have demonstrated that intense optical pulses can be used to efficiently modulate photoelectric absorption for x-rays in spite of rapid population decay inherent to core-excited states. The optical pulse dresses the final states of the x-ray transition; therefore the induced transparency is not due to hole burning or ground state bleaching. Our study represents a new strong-field regime for the formation of Autler-Townes-like structures in absorption spectra. This regime, relevant to x-ray wavelengths, is characterized by coherent strong coupling between short-lived core-excited states and a requirement of intense control beams to combat rapid population decay. Strong mixing of core-excited Rydberg levels and laser-induced ionization are unavoidable consequences of high control-beam intensity, and these mechanisms introduce complexities not typically encountered at longer wavelength. A reversible, ultrafast transmission switch was demonstrated which permits the measurement of the temporal duration of a femtosecond x-ray pulse. Theoretical simulations for gas-phase neon were shown to have excellent predictive power.

An application of the optical control demonstrated here is to imprint ultrafast laser pulse sequences onto long x-ray pulses as available at synchrotron sources [18]. Indeed, one can imagine using multiple optical control pulses in multicomponent media to achieve spectral and temporal control over a wide x-ray bandwidth. Since the dominant timescale is intra-atomic inner shell decay, extension of optical control of x-ray absorption to condensed phase and molecular systems may be feasible. Furthermore, the ability to optically control x-ray absorption on the ultrafast timescale may allow the

exciting prospect of tuning the relative importance of absorption and scattering. Quantum control in the x-ray regime has been demonstrated here. The next frontier includes the use of intense free-electron lasers for nonlinear x-ray spectroscopy and experiments where x-rays are used as both control and probe pulses.

Methods

Apparatus

Co-located sources of tunable short-pulse x-ray and high-intensity optical radiation are required for these experiments. The current experiments in neon in the soft x-ray regime can, to our knowledge, be performed at only three synchrotron-based laser-slicing facilities worldwide [29-31].

Experiments were performed at the Femtosecond Spectroscopy Beamline of the Advanced Light Source (ALS) [27,29]. See Figure 6. The soft x-ray branchline (6.0.2) can provide femtosecond duration pulses (~ 225 fs) tunable from ~0.2-2 keV at an average flux of 10^5 photons/sec*0.1% BW. Here, we produced femtosecond x-ray pulses at a 1 kHz repetition rate by laser interaction with the isolated camshaft bunch containing ~8 mA. X-rays were monochromatized ($\sigma_{instrument}$ = 0.22 eV) and focused to the center of a ~2 cm long, differentially-pumped gas cell containing 40 or 80 torr of Ne. Co-propagating dressing-laser pulses (800 nm, 1.1 mJ, 290 fs, 500 Hz) were synchronized to the ALS storage ring on a ~2 ps timescale. Since a single laser oscillator generated both femtosecond x-ray and optical pulses, the finite laser/storage-ring jitter (~ 2 ps) caused small (< 1%) x-ray amplitude fluctuations rather than timing jitter between optical and x-ray pulses; the effective synchronization between optical and x-ray pulses was better than 100 fs.

The gas cell, spatial and temporal overlap tools were located on an xyz-translation stage. Transmitted laser and x-ray pulses were detected downstream. Knife-edge scans were used to determine the overlap of optical and x-ray pulses with

~micron precision. An *in situ* metal-semiconductor-metal (MSM) photodiode provided a starting point for temporal overlap good to ~3 ps. Optical pulses propagated nearly collinearly (~11 mrad crossing angle) with x-ray pulses, but had a vertical offset of 48 μm. The laser focus varied through the 2 cm gas cell with a minimum size of $\sigma_{horizontal}$ = 34 μm, $\sigma_{vertical}$ = 68 μm. The x-rays were focused to a minimum size of $\sigma_{horizontal}$ = 23 μm, $\sigma_{vertical}$ = 36 μm. The maximum coupling laser intensity seen by x-ray excited atoms was 2.5×10^{13} W/cm^2.

Sliced x-ray pulses were generated at 1 kHz while laser-dressing pulses were generated at 500 Hz. Sliced x-ray pulses sequentially propagated through the gas target in the presence and absence of the control laser pulses to combat long term drift. Backgrounds were measured one storage ring period (656 ns) later. After a suitable data acquisition period (~10 s) the x-ray energy (time delay) was stepped to acquire a spectrum (cross-correlation). X-ray transmission was recorded with an avalanche photodiode located ~1-m downstream of the gas cell on a pulse-by-pulse basis. The avalanche photodiode was operated in photon counting mode and the resulting transmission spectra were corrected for multiple counting assuming Poisson statistics. The laser-dressed and laser-free transmission spectra were computed after subtraction of backgrounds. All error bars are statistical.

Simulations

The measured x-ray and laser pulse spatial and temporal properties and trajectories were input to a propagation code. X-ray propagation calculations were

necessary because the gas density in the cell was so high that, even if the x-ray absorption cross section in the interaction volume were constant, the transmitted x-ray intensity would not be a linear function of the x-ray absorption cross section. The propagation code calculated x-ray transmission at each space-time point as the x-ray and laser pulses traversed the neon medium. Interpolation of *ab initio* data [18,21,22] for 32 laser intensities between 0.5×10^{11} – 3×10^{13} W/cm^2 defined the x-ray absorption cross section for the laser intensity at each space-time point. The x-ray pulse was represented on a spatial grid consisting of 41×41 points transverse to and 51 points along the propagation direction covering 3.5 FWHMs in each direction. The x-ray pulse was propagated through the cell in 3900 time steps of 15.75 fs duration assuming monochromatic x-ray radiation for energies between 864 – 875 eV in 0.02 eV steps. The properly weighted transmission for a given central x-ray energy, due to the monochromator bandwidth, was computed *a posteriori.*

Acknowledgements

We thank C. Buth and S.E. Harris for enlightening discussions and D.L. Ederer, T. Weber, R.W. Schoenlein, and P. Heimann for experimental support during early stages of this project. This work was supported by the Chemical Sciences, Geosciences, and Biosciences Division of the Office of Basic Energy Sciences, Office of Science, U.S. Department of Energy, under Contract No. DE-AC02-06CH11357 and DE-AC02-05CH11231. This work was performed at the Advanced Light Source, Lawrence Berkeley National Laboratory, and was supported by the Office of Science, Office of Basic Energy Sciences, of the U.S. Department of Energy under Contract No. DE-AC02-05CH11231.

Author Contributions

TEG, MPH, AB, SHS, LY contributed to the design of the experiment. TEG, MPH, BR were responsible for the femtosecond x-ray beamline and control laser performance. TEG, MPH, SHS, TKA, JVT, EPK, BK, and LY collected the data. HRV and RS performed supporting theoretical calculations. Data analysis and interpretation were done by SHS, TEG, MPH, EPK, RS, and LY.

Competing Financial Interests

The authors declare no competing financial interests.

Additional Information

Correspondence and requests for materials should be addressed to L.Y.

References

[1] Cavalleri, A. *et al*. Band-Selective Measurements of Electron Dynamics in VO_2 Using Femtosecond Near-Edge X-ray Absorption. *Phys. Rev. Lett.* **95**, 067405 (2005).

[2] Fritz, D.M. *et al.* Ultrafast Bond Softening in Bismuth: Mapping a Solid's Interatomic Potential with X-rays. *Science* **315**, 633-636 (2007).

[3] Bressler, Ch., *et al.* Femtosecond XANES Study of the Light-Induced Spin Crossover Dynamics in an Iron (II) Complex.*Science* **323**, 489-492 (2009).

[4] Chen, L. X. Taking Snapshots of Photoexcited Molecules in Disordered Media by Using Pulsed Synchrotron X-rays, *Angewandte Chemie International Edition* **43**, 2886-2905 (2004).

[5] Bressler, C. & Chergui, M. Ultrafast X-ray Absorption Spectroscopy. *Chemical Reviews* **104**, 1781-1812 (2004).

[6] Hertlein, M.P. *et al.* Inner-shell ionization of potassium atoms ionized by a femtosecond laser. *Phys. Rev. A.* **73**, 062715 (2006).

[7] Young, L. *et al.* X-Ray Microprobe of Orbital Alignment in Strong-Field Ionized Atoms. *Phys. Rev. Lett.* **97**, 083601 (2006).

[8] Peterson, E. R. *et al.* An x-ray probe of laser aligned molecules, *Appl. Phys. Lett.* **92**, 094106-1-3 (2008).

[9] Harris, S.E. Electromagnetically Induced Transparency. *Physics Today* No. 7 July, 36-42 (1997).

[10] Fleischhauer, M., Imamoglu, A. & Marangos, J.P. Electromagnetically induced transparency: Optics in coherent media. *Rev. Mod. Phys.* **77**, 633-673 (2005).

[11] Harris, S.E. Nonlinear optics at low light levels. *Phys. Rev. Lett.* **82**, 4611-4614 (1999).

[12] Loh, Z.H., Greene, C.H. & Leone, S.R. Femtosecond induced transparency and absorption in the extreme ultraviolet by coherent coupling of the He 2s2p ($^1P^0$) and $2p^2$ ($^1S^e$) double excitation states with 800 nm light. *Chem. Phys.* **350**, 7-13 (2008).

[13] Arthur, J. *et al.* Linac Coherent Light Source (LCLS) Design Study Report, SLAC report No. SLAC-R-593, UC-414, (2002).

[14] Altarelli, M. *et al.* DESY Report No. 2006-097, (2006)

[15] Tanaka, T. & Shintake, T. SCSS X-FEL Conceptual Design Report, RIKEN Harima Institute/ Spring-8, 2005.

[16] DeCamp, M. F. *et al.* Coherent control of pulsed X-ray beams. *Nature* **413**, 825-828 (2001).

[17] Grigoriev, A. *et al.* Subnanosecond piezoelectric x-ray switch. *Appl. Phys. Lett.* **89**, 021109 (2006).

[18] Buth, C., Santra, R., & Young, L. Electromagnetically Induced Transparency For X-rays. *Phys. Rev. Lett.* **98**, 253001-1-4(2007).

[19] Brumer, P.W. & Shapiro, M. *Principles of the Quantum Control of Molecular Processes.* John Wiley & Sons, Inc., Hoboken, New Jersey (2003).

[20] Schweigert, I.V. & Mukamel, S. Coherent Ultrafast Core-Hole Correlation Spectroscopy: X-ray Analogues of Multidimensional NMR. *Phys. Rev. Lett.* **99**, 163001 (2007).

[21] Varma, H. R., Pan, L., Beck, D.R. & Santra, R. X-ray absorption near-edge structure of laser-dressed neon, *Phys. Rev. A* **78**, 065401:1-4 (2008).

[22] Buth, C. & Santra, R. Theory of x-ray absorption by laser-dressed atoms, *Phys. Rev. A* **75**, 033412:1-12 (2007).

[23] Autler, S.H. & Townes, C.H. Stark Effect in Rapidly Varying Fields. *Phys. Rev.* **100**, 703-722 (1955).

[24] Littman, M.G., Kash, M.M. & Kleppner, D. Field-Ionization Processes in Excited Atoms. *Phys. Rev. Lett.* **41**, 103-107 (1978).

[25] Agrawal, G.S. Nature of the quantum interference in electromagnetically-field-induced control of absorption. *Phys. Rev. A* **55**, 2467-2470 (1997).

[26] Imamoglu, A., & Harris, S.E. Lasers without inversion : interference of dressed lifetime-broadened states. *Opt. Lett.* **14**, 1344-1346 (1989).

[27] Steier, C. *et al.* Successful Completion of the Femtosecond Slicing Upgrade at the ALS. *Particle Accelerator Conference, PAC. IEEE* **25-29**, 1194-1196 (2007).

[28] See for example, Meyer, M. *et al.* Two-color photoionization in xuv free-electron and visible laser fields. *Phys. Rev. A* 74, 011401(R):1-4 (2006).

[29] Schoenlein, R.W. *et al.* Femtosecond pulses of synchrotron radiation: A new tool for ultrafast time-resolved x-ray spectroscopy. Science **287**, 2237-2240 (2000).

[30] Khan, S. *et al.* Femtosecond Undulator Radiation from Sliced Electron Bunches, *Phys. Rev. Lett.* **97**, 074801-1-4 (2006).

[31] Beaud, P. *et al.* Spatiotemporal Stability of a Femtosecond Hard–X-Ray Undulator Source Studied by Control of Coherent Optical Phonons. *Phys. Rev. Lett.* **99**, 174801-1-4 (2007).

[32] Coreno, M. *et al.* Measurement and *ab initio* calculation of the Ne photoabsorption spectrum in the region of the K edge. *Phys. Rev. A* **59**, 2492-2497 (1999).

Figure Captions

Figure 1. Relevant atomic states contributing to x-ray absorption. (a) Laser-free. A 1s → np Rydberg series and continuum threshold is observed. (b) In the presence of a strong coupling laser (ω_L). The dipole-allowed, x-ray active |np> manifold is mixed with the ns, nd … manifolds by the strong coupling laser. The x-ray absorption spectrum is further broadened by laser-induced ionization of the core-excited Rydberg levels. Only the lowest unoccupied s, p and d orbitals are shown in the diagram for simplicity, but an entire Rydberg series for each angular momentum manifold exists.

Figure 2. X-ray absorption spectrum for Ne in the absence of a coupling laser. Experimental data (markers) were obtained with femtosecond x-ray pulses from the ALS slicing source. The error bars indicate 1σ statistical uncertainties for data collection of 40s/pt. The solid line shows the convolution of the high resolution experimental Ne absorption spectrum from Coreno *et al.* [32] with a Gaussian instrument function (σ = 0.22 eV). The core to Rydberg transitions are labeled, and the inset shows the selected Λ-system (1s,3p,3s) coupled by the optical laser and x-rays in the parallel polarization configuration ($\boldsymbol{\varepsilon}_L||\boldsymbol{\varepsilon}_X$). An optical laser (~1.55 eV) coherently couples core-excited 3s and 3p states ($\Delta_{3s\text{-}3p}$~1.88 eV), thereby inducing transparency on the 1s→3p x-ray absorption resonance.

Figure 3. The fractional change in x-ray transmission induced by the coupling laser in the parallel polarization configuration ($\boldsymbol{\varepsilon_L||\varepsilon_X}$) . Data are shown for three peak laser intensities of 2.5 x 10^{13} W/cm^2, 1.8 x 10^{13} W/cm^2, and 1.1 x 10^{13} W/cm^2 for a Ne target thickness of 108 torr-cm. At the highest intensity, x-ray transmission is increased by factor of 3. The error bars indicate 1σ statistical uncertainties for data collection of 20s/pt. The solid lines show theoretical simulations of the expected change in transmission obtained by co-propagating the imperfectly overlapped dressing laser and x-ray pulses through neon gas. (See Simulations sub-section.) The degree of transparency varies linearly with intensity within error.

Figure 4. Polarization dependence of the fractional change in x-ray transmission (left) and the calculated x-ray absorption cross section for laser-dressed neon (right). (a) Observed fractional change in x-ray transmission, for a laser-dressed Ne target of thickness 54 torr-cm. Top: parallel polarization ($\boldsymbol{\varepsilon_L||\varepsilon_X}$). Bottom: perpendicular polarization ($\boldsymbol{\varepsilon_L\perp\varepsilon_X}$). The error bars indicate 1σ statistical uncertainties for data collection of 80s/pt. The solid lines show theoretical simulations. (See Simulations subsection.) Coherent coupling between 3s and 3p states, which modifies x-ray transmission, is allowed for parallel laser/x-ray polarizations only. The dramatic (~5x) dependence on polarization indicates that optically induced 3s-3p coherence is the primary mechanism causing the strong transparency observed for parallel polarization. (b) *Ab initio* x-ray absorption cross sections of neon with a 10^{13} W/cm^2, 800-nm dressing laser (blue) and laser-free (red). Top: parallel polarization ($\boldsymbol{\varepsilon_L||\varepsilon_X}$). Bottom:

perpendicular polarization ($\boldsymbol{\varepsilon}_L \perp \boldsymbol{\varepsilon}_X$). The polarization dependence of the laser-dressed absorption cross sections of neon at a single intensity indicates the origin of the optically induced x-ray transparency.

Figure 5. Cross-correlation measurement of the femtosecond x-ray pulse duration from the ALS slicing source. An x-ray and a dressing laser pulse, with variable delay, co-propagate through the gas cell. Positive delay corresponds to an x-ray pulse arriving after a laser pulse. Transmitted x-rays are detected by an avalanche photodiode. X-rays are tuned to the 1s→3p field-free absorption maximum at 867.1 eV and an x-ray/optical cross-correlation is obtained by measuring the increase in the transmitted x-ray flux as a function of delay. The correlation width (~380 fs) and measured laser duration (~290 fs) indicate an x-ray duration of ~250 fs. The error bars indicate 1σ statistical uncertainty.

Figure 6. Layout of the Femtosecond Spectroscopy Beamline at the Advanced Light Source. Femtosecond x-ray and laser pulses were derived from a single 800 nm laser oscillator. Their relative jitter is estimated to be <100 fs. Femtosecond x-rays are produced via interaction of a laser pulse with an electron bunch as it passes through an insertion device. Beamline optics monochromatize, focus and direct the x-rays to the experimental setup. Laser pulses (800 nm, 1.1 mJ, 290 fs) were focused to attain the requisite dressing intensity (~10^{13} W/cm^2) . The polarization and delay of the laser pulses relative to the x-ray pulses were controlled by a waveplate and delay stage. The x-ray and laser pulses co-propagated through the neon gas cell. The transmitted x-ray

intensity was detected by an avalanche photodiode operated in photon counting mode and recorded on a pulse-by-pulse basis.

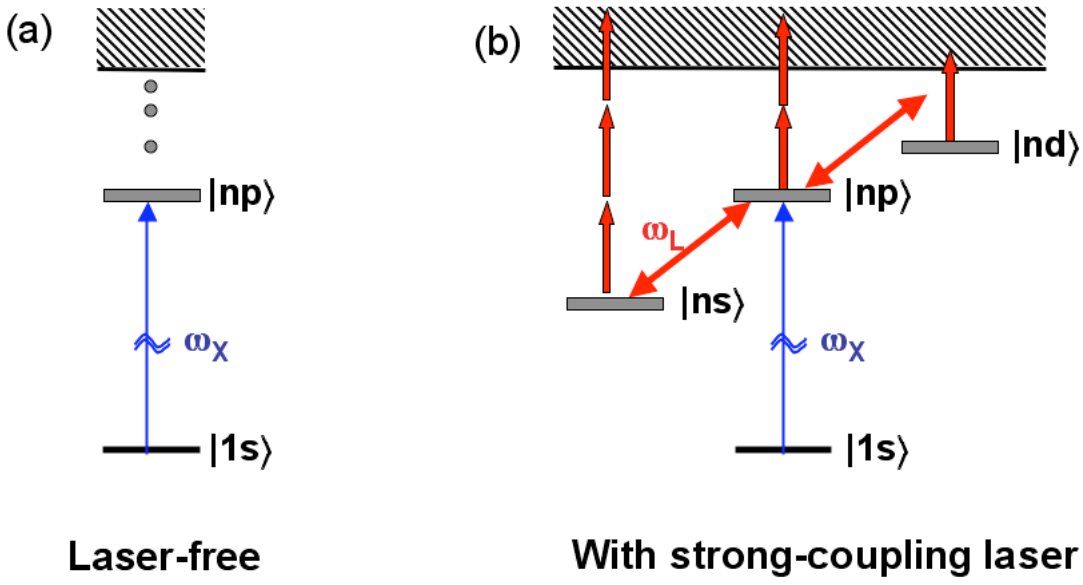
(a)
|np⟩
ωX
|1s⟩
Laser-free
(b)
|nd⟩
|np⟩
ωL
|ns⟩
ωX
|1s⟩
With strong-coupling laser

Figure 1

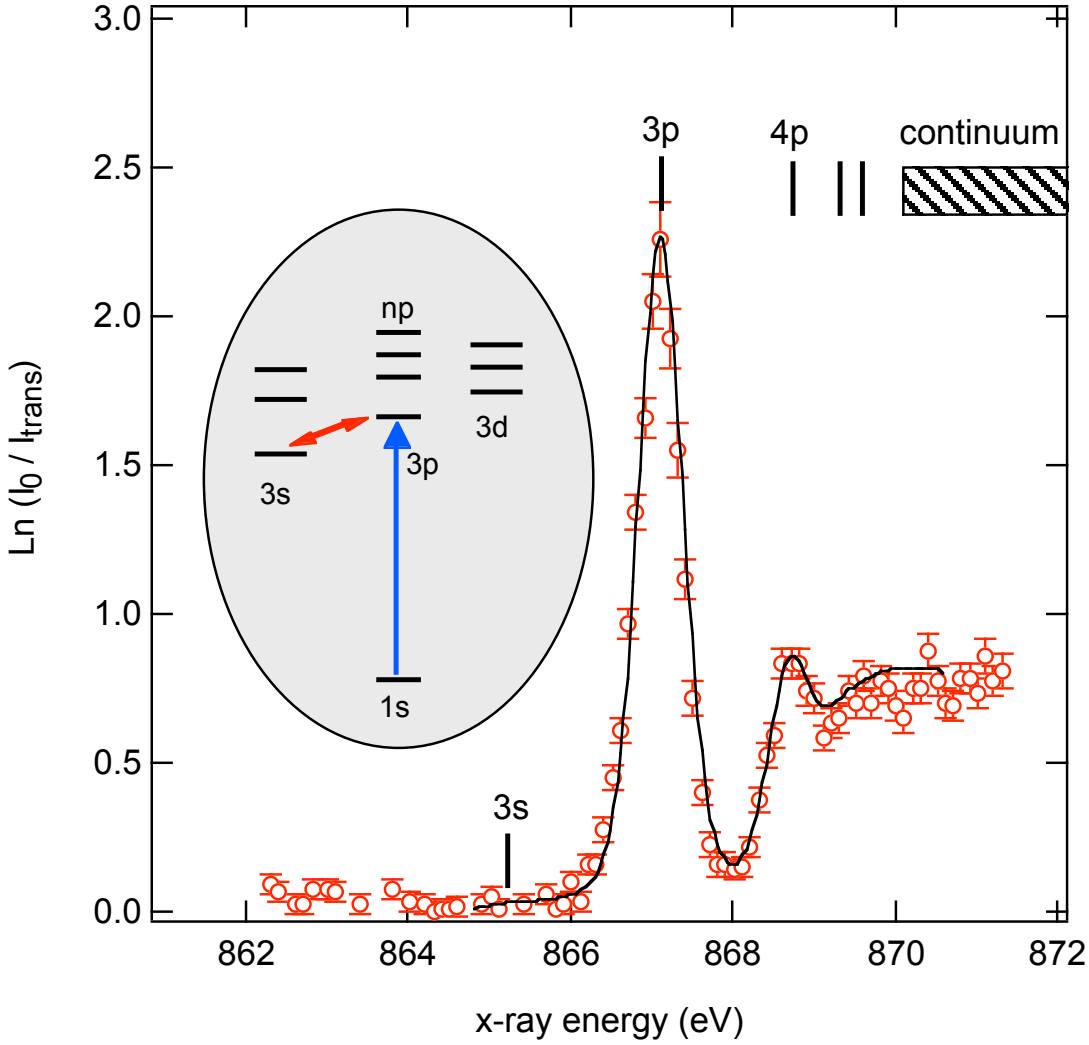
3.0
2.5
2.0
1.5
1.0
0.5
0.0
Ln (I0 / Itrans)
862
864
866
868
870
872
x-ray energy (eV)
3p
4p
continuum
3s
np
3d
3p
1s
3s

Figure 2

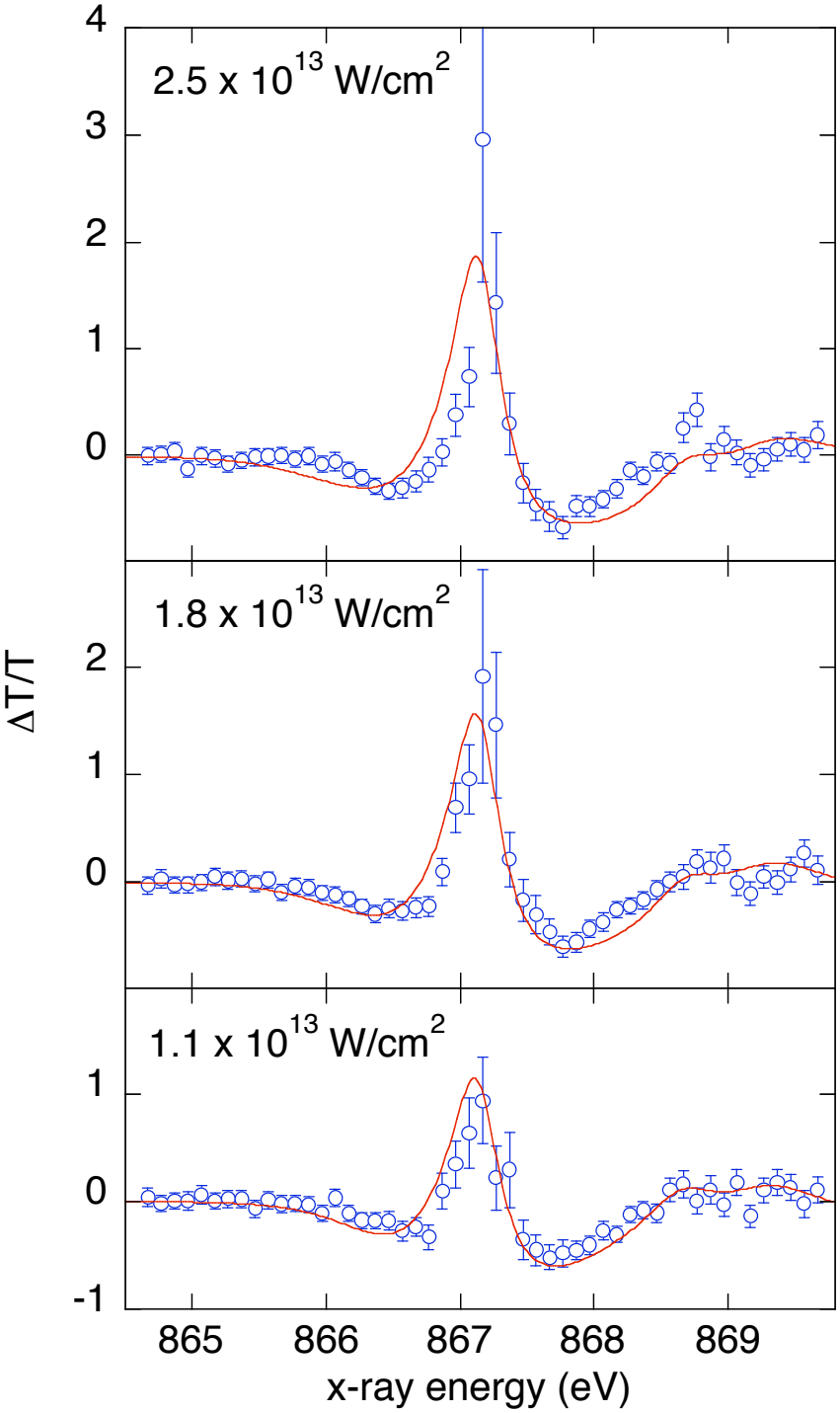
2.5 x 10^13 W/cm^2
1.8 x 10^13 W/cm^2
1.1 x 10^13 W/cm^2
ΔT/T
x-ray energy (eV)
865
866
867
868
869

Figure 3.

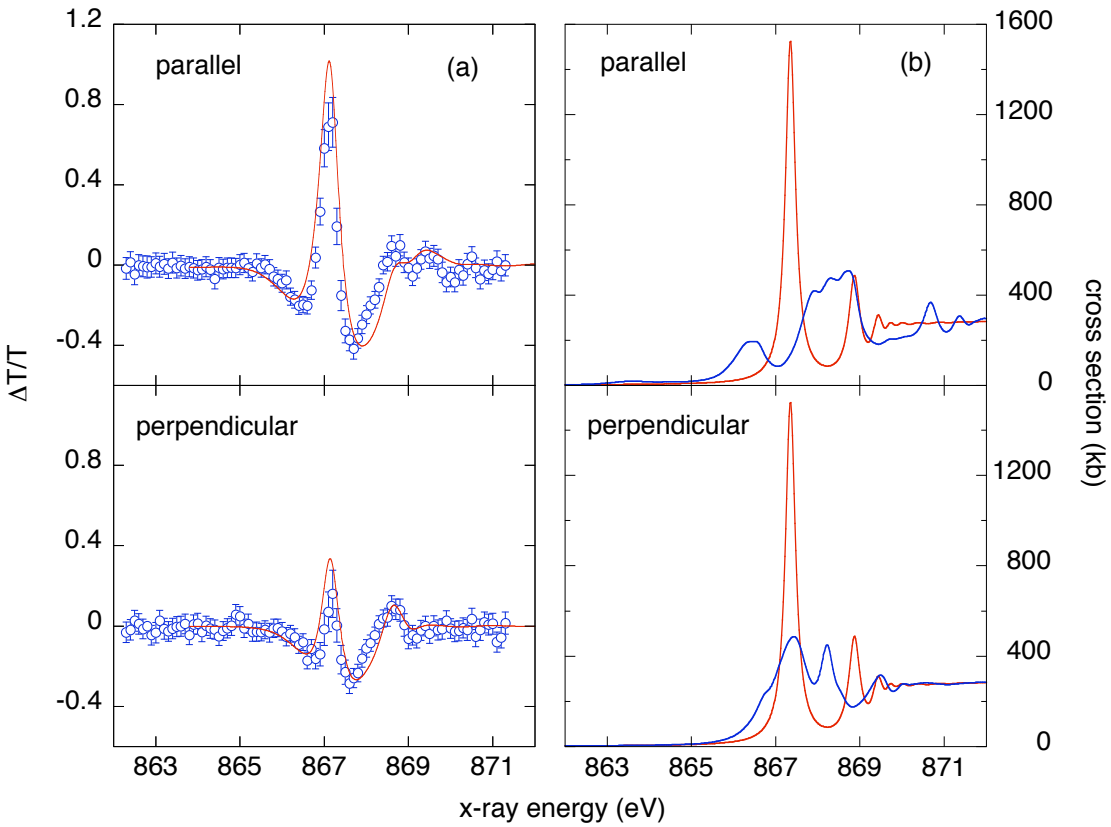
parallel
(a)
parallel
(b)
perpendicular
perpendicular
ΔT/T
cross section (kb)
x-ray energy (eV)
1.2
0.8
0.4
0
-0.4
1600
1200
800
400
0
863
865
867
869
871

Figure 4.

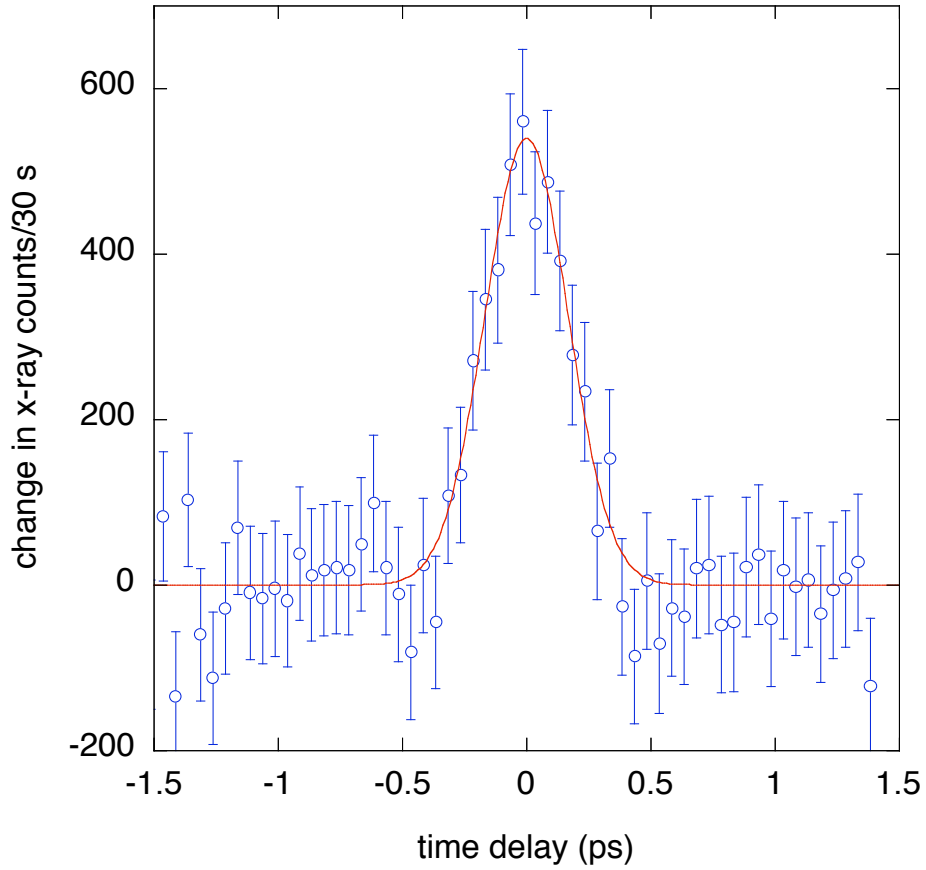
600
400
200
0
-200
change in x-ray counts/30 s
-1.5
-1
-0.5
0
0.5
1
1.5
time delay (ps)

Figure 5

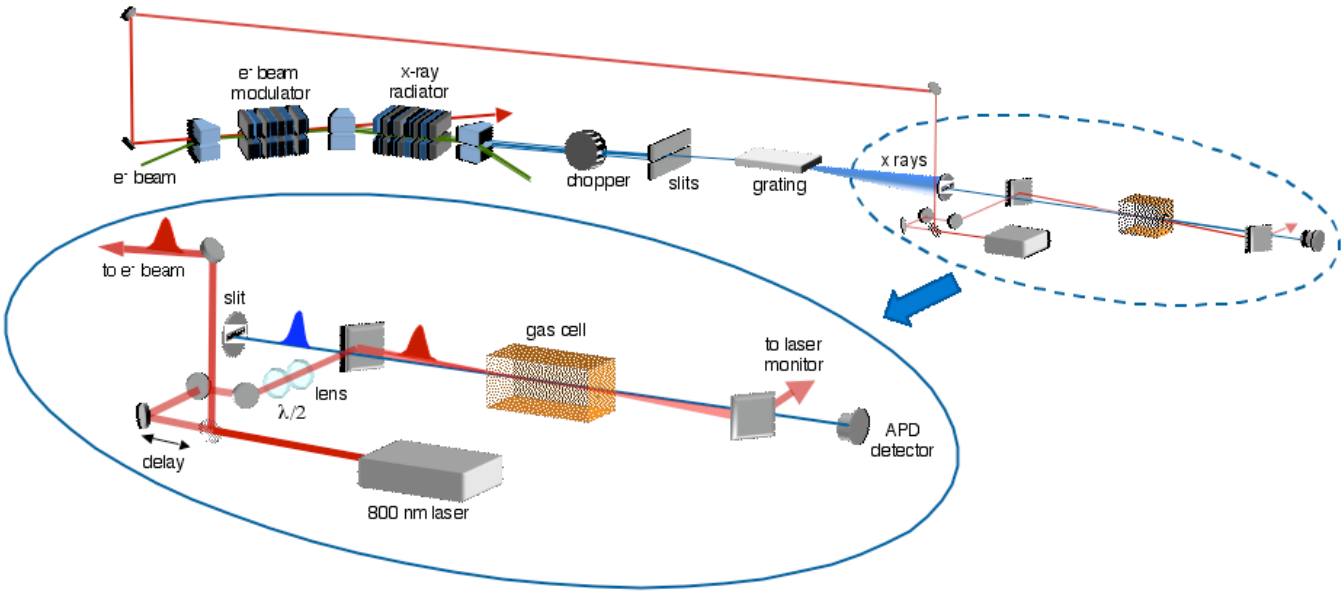
e⁻ beam
modulator
x-ray
radiator
e⁻ beam
chopper
slits
grating
x rays
to e⁻ beam
slit
gas cell
to laser
monitor
lens
λ/2
APD
detector
delay
800 nm laser

Figure 6.